International Journal of Solids and Structures 51 (2014) 4435–4439

Contents lists available at ScienceDirect

International Journal of Solids and Structures

journal homepage: www.elsevier.com/locate/ijsolstr

Contact problems involving beams

Jae Hyung Kim [a], Young Ju Ahn [b], Yong Hoon Jang [a], J.R. Barber [c,*]

[a] School of Mechanical Engineering, Yonsei University, Shincheon-Dong 134, Seodaemun-Gu, Seoul 120-749, Republic of Korea
[b] Department of Mechanical and Design Engineering, Hongik University, Sejong-si 339-701, Republic of Korea
[c] Department of Mechanical Engineering, University of Michigan, Ann Arbor, MI 48109-2125, USA

ARTICLE INFO

Article history:
Received 21 July 2014
Received in revised form 10 September 2014
Available online 28 September 2014

Keywords:
Contact problems
Beams
Plates
Finite element methods
Asymptotic methods

ABSTRACT

Elastic contact problems involving Euler–Bernoulli beams or Kirchhoff plates generally involve concentrated contact forces. Linear elasticity (e.g. finite element) solutions of the same problems show that finite contact regions are actually developed, but these regions have dimensions that are typically of the order of the beam thickness. Thus if beam theory is appropriate for a given structural problem, the local elasticity fields can be explored by asymptotic methods and will have fairly general (problem independent) characteristics. Here we show that the extent of the contact region is a fixed ratio of the beam thickness which is independent of the concentrated load predicted by the beam theory, and that the distribution of contact pressure in this region has a universal form, which is well approximated by a simple algebraic expression.

1. Introduction

If classical Euler–Bernoulli beam theory is used to describe elastic components in frictionless contact, the solutions generally predict concentrated contact forces — i.e. that the extent of the contact area is restricted to one or more isolated points. A simple example is illustrated in Fig. 1, where a beam of length L is simply supported at its ends, and a rigid cylinder of radius R is pressed against it at the mid point by a force P.

In this situation, contact will occur only at the mid-point as long as the radius of curvature of the deformed beam is greater than R and this condition is satisfied if

$$P < P_0 \equiv \frac{4EI}{LR}, \tag{1}$$

where EI is the flexural rigidity of the beam.

For $P > P_0$, a finite strip of contact is developed — i.e. the beam conforms to the shape of the cylinder over a line segment of length a, but non-zero tractions are limited to a pair of concentrated forces $P/2$ at the two edges of this segment (Johnson, 1985), as shown in Fig. 2. The beam is then essentially loaded in 'four-point bending' and the bending moment in the contact segment is $P(L-a)/4$, corresponding to a radius of curvature $4EI/P(L-a)$. Equating this to the radius of the cylinder and solving for the length a, we obtain

$$a = L - \frac{4EI}{PR} = L\left(1 - \frac{P_0}{P}\right). \tag{2}$$

1.1. Higher order beam theories

Clearly the continuum solution of this problem will not involve concentrated forces, with the corresponding implication of locally unbounded stresses and strains. Instead, we anticipate the development of small but finite regions of contact with correspondingly large local contact stresses, whose value may be of importance for design purposes.

Some degree of regularization in the beam solution can be achieved by using higher order theories, such as Timoshenko beam theory (Chen, 2011), or by including the effect of transverse normal strain (Naghdi and Rubin, 1989; Gasmi et al., 2012). However, the resulting theories are considerably more complex to apply, and the contact pressure distributions still exhibit significant deviations from the 'exact' solution, particularly at the edges of the predicted contact region, where asymptotic arguments require that the contact pressure should go to zero with a square-root bounded form (Johnson, 1985).

1.2. Analytical solutions

The problem of Fig. 1 was solved exactly in the context of elasticity theory by Keer and Miller (1983), by expressing the elastic fields in the beam as Fourier transforms with respect to

* Corresponding author. Tel.: +1 734 936 0406.
E-mail address: jbarber@umich.edu (J.R. Barber).

http://dx.doi.org/10.1016/j.ijsolstr.2014.09.013
0020-7683/

the horizontal variable. The lower surface of the beam is traction-free, and because the contact conditions are frictionless, the shear traction on the upper surface is also zero everywhere. Thus, three of the four boundary conditions are 'global' and can be satisfied by elementary relations between the transform variables. The remaining (normal) conditions on the upper surface then lead to a pair of dual integral equations and these can be reduced to a single Fredholm equation that must be solved numerically.

1.3. Finite element solutions

The Fourier transform technique has been applied to a range of beam-like contact problems (Schonberg et al., 1987; Keer and Schonberg, 1986; Keer and Silva, 1972) of which it clearly represents the definitive solution. However, its use demands a significant familiarity with dual integral equations and the final calculation still involves a numerical solution. A more straightforward alternative is of course to solve the complete structural contact problem using a two or three-dimensional finite element model, in which the contact tractions can be approximated to any desired degree of accuracy by suitable mesh refinement. However, this approach has its own problems, notably because (i) the resulting contact areas are very small and hence require very fine local meshing, but (ii) in many cases (for example, for the problem of Fig. 1 with $P > P_0$), the exact location of the contact region is not known *a priori*, so this fine mesh may need to be extended over a substantial region of the body.

1.4. Asymptotic arguments

The fact that the local contact stress fields will be restricted to a region that is small compared with the other dimensions of the problem opens up the possibility of using asymptotic methods. These methods have been used to great effect in deducing the character of the local frictional slip zones and stress fields in fretting fatigue applications, from parameters defined in the simpler, fully adhered solution (Churchman and Hills, 2006; Flicek et al., 2013).

In the problem of Fig. 1, if we choose a coordinate system centered on one of the two contact regions implied by the geometry of Fig. 2, and magnify the scale sufficiently for the resulting finite contact area to occupy most of the field of interest, then the magnification will usually be sufficient for the ends of the beam and the other region of contact to appear a large distance away. St. Venant's principle then suggests that the effects of these distant loads can influence the local contact region only through the local values of bending moment and shear force, and hence it should be possible to characterize the local contact fields in terms of a quite limited number of parameters. In other words, we should be able to develop a few fairly general continuum contact solutions that can be 'patched in' to beam contact problems, enabling the maximum contact pressure and other parameters of interest to be predicted without necessitating a full continuum solution of the each individual problem. This is the objective of the present paper.

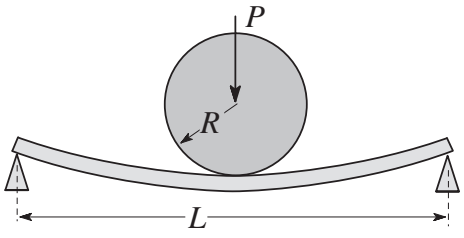

Fig. 1. A cylinder pressed against a beam.

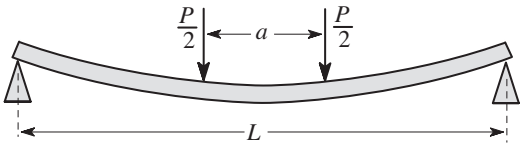

Fig. 2. Contact tractions for $P > P_0$.

2. Hertzian approximation

We consider the two-dimensional plane strain problem in which the beam of Figs. 1 and 2 is of depth h and the force P is to be interpreted as force per unit length (into the paper). We then have

$$EI = \frac{E^* h^3}{12} \quad \text{and} \quad P_0 = \frac{E^* h^3}{3LR}, \tag{3}$$

where

$$E^* = \frac{E}{(1-\nu^2)} \tag{4}$$

is the plane strain modulus, and E, ν are Young's modulus and Poisson's ratio respectively.

If $P \ll P_0$, it seems reasonable to expect that the local contact behavior in Fig. 1 will be well approximated by the Hertzian equations. In particular, that the contact pressure distribution will be given by (Johnson, 1985)

$$p(x) = \frac{2P\sqrt{b^2 - x^2}}{\pi b^2} \tag{5}$$

and the contact semi-width b will be

$$b = 2\sqrt{\frac{PR}{\pi E^*}}. \tag{6}$$

We might hope to obtain a better approximation to the local fields by recognizing that in the beam solution, the contact surface is concave with radius

$$R_b = \frac{4EI}{PL}. \tag{7}$$

This value is determined by the bending moment in the beam, which is only very slightly affected by the exact contact pressure distribution, so we can reasonably treat it as a pre-existing radius and calculate $p(x)$ and b by replacing R by the composite radius R^* where

$$\frac{1^*}{R} = \frac{1}{R} - \frac{1}{R_b} = \frac{1}{R}\left(1 - \frac{P}{P_0}\right). \tag{8}$$

We obtain

$$b = 2\sqrt{\frac{h^3}{3\pi L}\left(\frac{\tilde{P}}{1-\tilde{P}}\right)} \quad \text{where} \quad \tilde{P} = \frac{P}{P_0}, \tag{9}$$

after which $p(x)$ is given by (5). In particular, the maximum contact pressure is

$$p(0) = P_0\sqrt{\frac{3L\tilde{P}(1-\tilde{P})}{\pi h^3}}. \tag{10}$$

3. Finite element solution

To evaluate the range in which these approximations are appropriate, we constructed a finite element model of the problem. The

mesh was refined sufficiently to ensure that there were never less than 200 contact nodes in any contact region in the following results. The finite element model used 2,000,000 four-node isoparametric quadrilateral elements, with a total of 2,010,201 nodes for $h/L = 0.02$.

Fig. 3 compares the predictions of the contact semi-width b from Eq. (9) (solid line) with the finite element results for $h/L = 0.02$ (circles) and $h/L = 0.2$ (squares). The dashed line in this figure represents the simple Hertzian prediction (6). As we might expect, this gives a good approximation for very low values of P/P_0, but is not useful beyond about $P/P_0 = 0.2$. By contrast, Eq. (9) gives very accurate predictions for $P/P_0 < 0.5$ even for $h/L = 0.2$ which outside the range for which beam theory might be thought appropriate. For $h/L = 0.02$, the approximation is excellent up to $P/P_0 = 0.9$.

Fig. 4 shows a similar comparison for the maximum contact pressure $p(0)$. Notice in particular that the Hertzian theory predicts that $p(0)$ increases monotonically with P, but Eq. (10) correctly identifies the non-monotonic shape of the curve. Figs. 3 and 4 were computed using a radius $R = 2000h$ ($h/R = 0.0005$), but similar calculations using h/R in the range $(0.005, 0.0002)$ fall on the same curve, showing that in the linear range at least, the results are independent of R.

3.1. Results for $P > P_0$

For $P > P_0$, the beam solution predicts two concentrated forces as shown in Fig. 2. The bending moment in the central segment is independent of a, so as long as $a \gg h$ — i.e. the two contact points are sufficiently far apart for their local fields not to interact — the only parameter defining the local field is the magnitude of the predicted concentrated force $P/2$. Furthermore, the concentrated force defines a perturbation from pure bending that is independent of the local bending moment, suggesting that the local field will be independent of the radius R for a given value of $P/2$.

The finite element results show that the width b of each of the two contact regions is independent of P in the range $P > 2P_0$, being given by $b = 2.3h$ for sufficiently small values of h/R. Fig. 5 shows the dependence of b/h on h/R in this range and shows that there is no significant dependence on h/R below 10^{-3}. Fig. 6 shows the corresponding contact pressure distribution in the left contact area, normalized with respect to the average pressure F/b, where $F = P/2$ is the resultant force. The factor of 2 in this expression arises because each of the two concentrated forces in the beam solution is equal to $P/2$. The numerical results show that this normalized distribution is independent of P/P_0 in the range $P > 2P_0$.

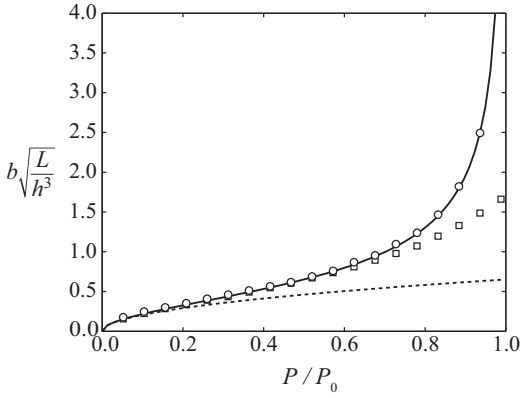

Fig. 3. Contact semi-width b for $P < P_0$. The solid line is defined by Eq. (9), the circles are for $h/L = 0.02$ and the squares for $h/L = 0.2$. The dashed line is the Hertzian solution (6).

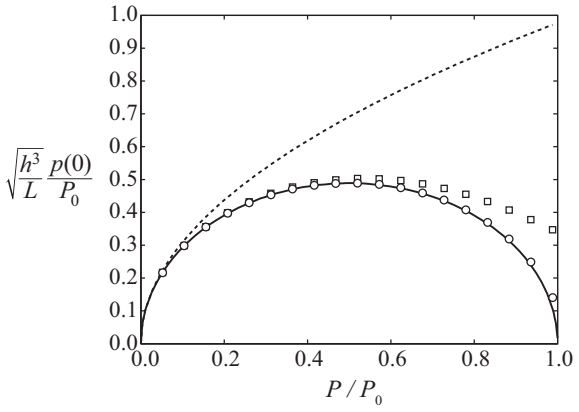

Fig. 4. Maximum contact pressure $p(0)$ for $P < P_0$. The solid line is defined by Eq. (9), the circles are for $h/L = 0.02$ and the squares for $h/L = 0.2$. The dashed line is the Hertzian solution (6).

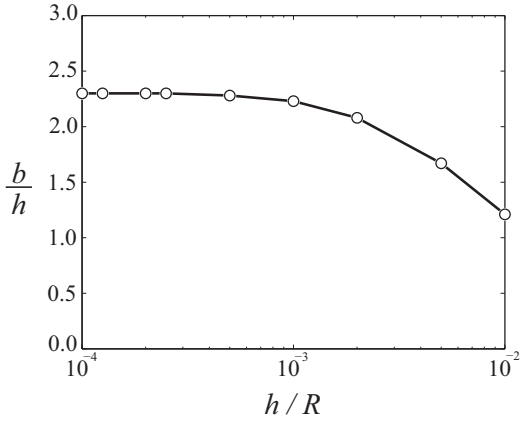

Fig. 5. Dependence of the contact width b on indenter radius R for $P > P_0$.

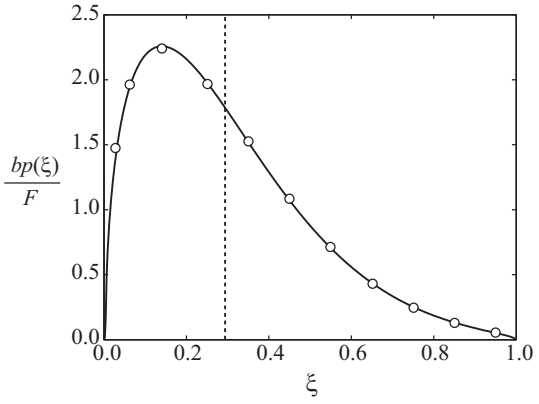

Fig. 6. Normalized contact pressure distribution at the left contact zone for $P > P_0$ (circles). The curve fit of Eq. (11) is shown as a solid line. The vertical dashed line defines the line of action of the resultant force.

An acceptable curve fit to these results, with the asymptotically required square-root bounded form at each edge of the contact area, is given by the expression

$$p(\xi) = \frac{F}{b}\left(C_0 + C_1\xi + C_2\xi^2 + C_3\xi^3\right)\sqrt{\xi(1-\xi)}, \tag{11}$$

where $\xi = x/b = x/2.3h$, x is measured from the edge of the separation zone, and $C_0 = 9.624$, $C_1 = -25.82$, $C_2 = 24.08$, $C_3 = -7.667$. This expression is shown as the solid line in Fig. 6.

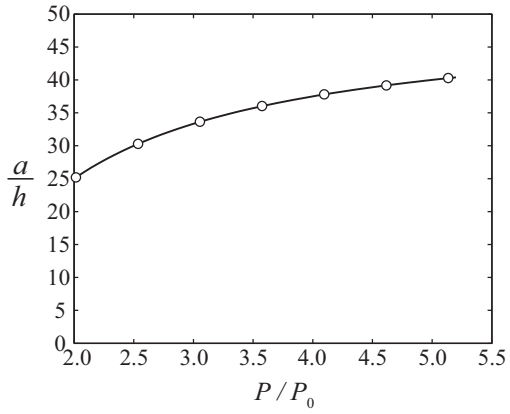

Fig. 7. Distance a between the lines of action of the two patches of contact pressure from the finite element solution (circles) for $P > P_0$. The solid line is defined by Eq. (2).

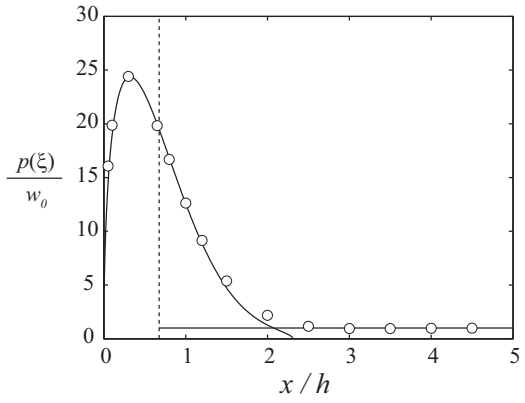

Fig. 9. Contact pressure distribution for the problem of Fig. 8 with $F = 25w_0h$.

The beam solution predicts that the two concentrated forces should be separated by a distance a given by Eq. (2). To compare with this, we computed the line of action of the resultant force corresponding to the pressure distribution of Fig. 6 and found the distance between the lines of action of the two forces in the finite element solution. The results are compared with the beam prediction in Fig. 7. The beam solution (solid line) is essentially indistinguishable from the finite element results, shown as circles. To put this result in perspective, we indicate by a vertical dashed line the location of the resultant force in Fig. 6, which acts through the point $\xi = c$, where $c = 0.294$. Alternatively, if we define a new coordinate x' measured from the location of the concentrated force in Fig. 2, the actual pressure distribution is well approximated by the expression (11) with $\xi = \xi' + c$ and $b = 2.3h$.

4. Example

The scientific value of the above results is that they can in principle be applied to any contact problem involving beams in which a concentrated contact force is predicted at the edge of a segment of contact. To illustrate this, we consider the problem shown in Fig. 8, in which a rectangular beam of depth h resting on a rigid plane is subjected to a uniform downward pressure w_0 per unit length and an upward end force F, tending to lift a segment of the beam from the support. Elementary beam calculations show that the separated segment should be of length $2F/w_0$ and that there should be a concentrated contact force, also of magnitude F, at the separation point. This problem is discussed by Feodosyev et al. (1977) using a beam theory including shear deformations, and an exact analytical solution is given by Keer and Silva (1972) using the Fourier transform method.

The solid line in Fig. 9 shows the contact pressure distribution predicted in this problem for the case $F = 25w_0h$, using the beam solution, but with the concentrated force 'regularized' using the expression (11). Notice that in contrast to the problem of Fig. 2, the beam solution in this case predicts a uniform contact pressure equal to w_0 per unit length to the right of point B, which corresponds to the dashed vertical line in Fig. 9. so Eq. (11) cannot be correct very close to B. However, this error is necessarily rather small if the ratio between the separated length a and the beam depth h is large enough for beam theory to be appropriate. The circles in this figure represent a direct finite element solution of the same problem and are very close to the predictions from the regularized beam theory, except in a small transition region. In particular, the predictions of the location and magnitude of the maximum contact pressure are extremely good. We anticipate similar levels of agreement for all problems of this general class.

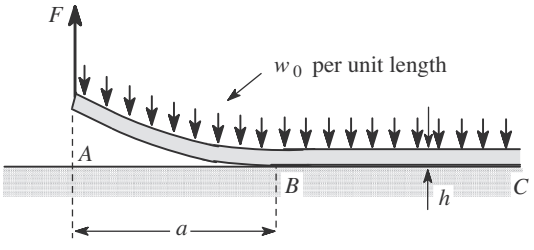

Fig. 8. A uniformly loaded beam lifted by an end force.

5. Three-dimensional problems

Similar problems arise in the contact of plates and shells. For example, if a rigid sphere is pressed into the center of a simply supported circular Kirchhoff plate by a force P, a concentrated line contact force will occur on a circle whose radius a increases with P. If $a/h \gg 1$, where h is the plate thickness, the three-dimensional solution of this problem will involve a finite contact pressure over a thin annulus near $r = a$ and we might expect the stress state to be locally approximately two-dimensional. Similar asymptotic methods have been used by Kalker (1977) to approximate the solution of three-dimensional contact problems involving slender contact areas, and a similar asymptotic argument underpins the use of stress-intensity factors as a measure of loading severity in three-dimensional fracture problems.

This argument leads us to expect the width of the annulus to be approximately $b = 2.3h$ and the pressure to take the form of Eq. (11), where the appropriate force per unit length from the plate solution is used for F.

6. Conclusions

The regularization introduced into contact problems for beams by the use of linear elasticity is localized to a region whose dimensions are of the order of the beam thickness. This implies that if beam theory is appropriate for a given structural problem, the local elasticity fields can be explored by asymptotic methods and will have fairly general (problem independent) characteristics. In particular, the extent of the contact region is a fixed ratio of the beam thickness which is independent of the load, and the distribution of contact pressure in this region has a universal form. This makes it possible to develop good approximations to the elasticity solution by (i) solving an equivalent beam or plate problem and then (ii)

patching in a local corrective field to regularize the resulting concentrated forces.

Acknowledgements

We are pleased to acknowledge support from the Basic Science Research Program through the National Research Foundation of Korea (NRF) funded by the Ministry of Education, Science and Technology (Y.H. Jang and J.H. Kim, Grant No. 2012R1A1A2042106), and the Ministry of Science ICT and Future Planning (Y.-J. Ahn, Grant No. 2014R1A1A1004186).

References

Chen, J.S., 2011. On the contact behavior of a buckled Timoshenko beam constrained laterally by a plane wall. Acta Mech. 222, 225–232.

Churchman, C.M., Hills, D.A., 2006. Slip zone length at the edge of a complete contact. Int. J. Solids Struct. 43, 2037–2049.

Feodosyev, V.I., 1977. Selected Problems and Questions in Strength of Materials. Mir, Moscow (Translated from the Russian by M. Konyaeva, (1977), Problem 59).

Flicek, R., Hills, D.A., Dini, D., 2013. Progress in the application of notch asymptotics to the understanding of complete contacts subject to fretting fatigue. Fatigue Fract. Eng. Mater. Struct. 36, 56–64.

Gasmi, A., Joseph, P.F., Rhyne, T.B., Cron, S.M., 2012. The effect of transverse normal strain in contact of an orthotropic beam pressed against a circular surface. Int. J. Solids Struct. 49, 2604–2616.

Johnson, K.L., 1985. Contact Mechanics. Cambridge University Press, Cambridge, p. 143.

Kalker, J.J., 1977. The surface displacement of an elastic half-space loaded in a slender bounded curved surface region with application to the calculation of the contact pressure under a roller. J. Inst. Math. Appl. 19, 127–144.

Keer, L.M., Miller, G.R., 1983. Smooth indentation of finite layer. ASCE J. Eng. Mech. 109, 706–717.

Keer, L.M., Schonberg, W.P., 1986. Smooth indentation of an isotropic cantilever beam. Int. J. Solids Struct. 22, 87–106.

Keer, L.M., Silva, M.A.G., 1972. Two mixed problems for a semi-infinite layer. ASME J. Appl. Mech. 39, 1121–1124.

Naghdi, P.M., Rubin, M.B., 1989. On the significance of normal cross-sectional extension in beam theory with application to contact problems. Int. J. Solids Struct. 25 (1989), 249–265.

Schonberg, W.P., Keer, L.M., Woo, T.K., 1987. Low velocity impact of transversely isotropic beams and plates. Int. J. Solids Struct. 23, 871–896.